STEM CELLS AND DEVELOPMENT
Volume 25, Number 22, 2016

DOI: 10.1089/scd.2016.0088

Contribution of Caudal Müllerian Duct Mesenchyme to Prostate Development

Hannah Brechka,[1] Erin M. McAuley,[2] Sophia M. Lamperis,[3] Gladell P. Paner,[4] and Donald J. Vander Griend[1,3]

A fundamental understanding of prostate development and tissue homeostasis has the high potential to reveal mechanisms for prostate disease initiation and identify novel therapeutic approaches for disease prevention and treatment. Our current understanding of prostate lineage specification stems from the use of developmental model systems that rely upon the embryonic preprostatic urogenital sinus mesenchyme to induce the formation of mature prostate epithelial cells. It is unclear, however, how the urogenital sinus epithelium can derive both adult urethral glands and prostate epithelia. Furthermore, the vast disparity in disease initiation between these two glands highlights key developmental factors that predispose prostate epithelia to hyperplasia and cancer. In this study we demonstrate that the caudal Müllerian duct mesenchyme (CMDM) drives prostate epithelial differentiation and is a key determinant in cell lineage specification between urethral glands and prostate epithelia. Utilizing both human embryonic stem cells and mouse embryonic tissues, we document that the CMDM is capable of inducing the specification of androgen receptor, prostate-specific antigen, NKX3.1, and Hoxb13-positive prostate epithelial cells. These results help to explain key developmental differences between prostate and urethral gland differentiation, and implicate factors secreted by the caudal Müllerian duct as novel targets for prostate disease prevention and treatment.

Keywords: androgen receptor, prostate, Müllerian duct, NKX3.1, HOXB13

Introduction

Prostate cancer and benign prostatic hyperplasia impact a significant cohort of men as they age. A fundamental understanding of prostate development and tissue homeostasis has the high potential to reveal mechanisms for prostate disease initiation and identify novel therapeutic approaches for disease prevention and treatment. In particular, it is essential to elucidate the contributions of cell types and key transcription factors involved in prostate development and cellular turnover, as many of these cell types and genes play key roles in disease initiation and progression.

It is well established that the prostate gland is derived from embryonic urogenital sinus (UGS), since UGS epithelial cells morphologically bud, branch, and canalize to form the prostate [1]. In addition to forming the prostate, however, UGS epithelial cells also develop into urethral glands, which are functionally distinct from HoxB13-positive mature prostate epithelial acini [2]. The human prostate is composed of multiple zones arranged symmetrically and includes the transition, central, and peripheral zones [3]. The peripheral zone is where most prostate cancer arises and the central zone wraps around the ejaculatory duct emerging from the seminal vesicle. The transition zone surrounds the urethra, which brings this zone into close proximity to periurethral glands. Urethral glands emerge along the urethra but are functionally and morphologically distinct from the surrounding prostate glands [4]. Paradoxically, while the prostate and urethral glands are derived from the same epithelial precursor cells, urethral gland epithelial cells rarely derive hyperplasia or cancer. This disparity highlights potential understudied mechanisms in prostate versus urethral gland epithelial development that make prostate epithelial cells more susceptible to disease initiation.

The current paradigm of prostate development provides a general explanation for how the UGS can give rise to multiple distinct regions and glands [1,5]. The cranial-caudal axis of the UGS allows for geographically distinct epithelial–mesenchymal interactions along the tissue. The differentiation and morphologic differences are controlled by temporal expression of distinct growth factors emerging from the mesenchyme. This primitive map allows regional identity of the adult glands in general, but there are gaps in knowledge about what factors are necessary for distinguishing urethral glands from prostatic glands.

[1]The Committee on Cancer Biology, [2]The Committee on Molecular Pathology and Molecular Medicine, [3]Department of Surgery, Section of Urology, and [4]Department of Pathology, The University of Chicago, Chicago, Illinois.

In this study we demonstrate that the caudal Müllerian duct mesenchyme (CMDM) is able to drive prostate epithelial differentiation and is a key determinant driving cell lineage specification between urethral glands and prostate epithelia. The CMDM is canonically associated with female urogenital development as the expression of anti-Müllerian hormone (AMH) in male sertoli cells causes the irreversible regression of the Müllerian Ducts in males [6,7]. However, the role of the Müllerian duct (MD) precursor tissue, the CMDM, has not been investigated in the context of the prostate. Utilizing both human embryonic stem cells (hESCs) and mouse embryonic tissues, we document that formation of androgen receptor (AR), prostate-specific antigen (PSA), NKX3.1, and HOXB13-positive prostate epithelial cells can be induced upon recombination with CMDM. These results help to explain key developmental differences between prostate and urethral gland differentiation, and provide support to investigate how factors secreted by the caudal MD may be involved in prostate disease prevention and treatment.

Materials and Methods

Human subjects

All human tissues were acquired under an expedited protocol approved by the University of Chicago Institutional Review Board (IRB). Tissue samples were managed by the University of Chicago Human Tissue Resource Center core facility.

Mice

Animal studies were carried out in strict accordance with the recommendations in the Guide for the Care and Use of Laboratory Animals of the National Institutes of Health and procedures were approved by the University of Chicago Institutional Animal Care and Use Committee. All mouse surgery was performed under Ketamine/Xylazine anesthesia, and all efforts were made to minimize animal suffering. Wild-type C57BL/6 mice were obtained from the Jackson Laboratory. Timed-pregnant C57BL/6 mice, 6-week-old male nude mice, and timed-pregnant Sprague Dawley rats were obtained from Harlan Laboratories (Indianapolis, IN).

Cell culture

The hESC line WA01(H1) was acquired from WiCell (Madison, WI) and cultured using the feeder-independent protocol using mTeSR1 media (Stem Cell Technologies; Vancouver, BC). The hESCs were used within 10 passages of thawing, and were dissociated using mTeSR1 media with an Accutase (Millipore; Billerica, MA) digestion.

Tissue recombination

Tissue recombination and renal grafting were performed using previously reported techniques and all recombination experiments were conducted in triplicate with appropriate controls [8]. In this study, the mesenchymal cells were derived from euthanized female newborn rats. The caudal MD, including the primordium of cervix and upper vagina, was separated from the UGS. The tissues were digested separately using 1% trypsin (BD Biosciences, San Joes, CA) in Ca^{2+} and Mg^{2+}-free Hank's balanced salt solution (HBSS; Gibco) and placed in a refrigerator at 4°C for 75 min. After neutralizing the trypsin with 10% fetal bovine serum (FBS) in Dulbecco's modified Eagle's medium (DMEM)/F12 medium (Gibco, Grand Island, NY), the mesenchymal sleeves were carefully teased from the epithelial tube. The CMDM and urogenital sinus mesenchyme (UGSM) were transferred into DMEM/F12 medium +10% FBS +1% Pen/Strep +1% NEAA plus 1 nM R1881 (Sigma, St. Louis, MO) and incubated at 37°C with 5% CO_2 overnight. After removing the culture medium, the mesenchyme was digested with 0.2% collagenase in DMEM/F12 medium and placed the tube in 37°C on a shaker for 1 h. The digested tissues were vigorously vortexed to yield a homogenous single cell suspension and collagen-neutralized using DMEM/F12 medium +10% FBS. The dissociated mesenchymal cells were washed with HBSS, and suspended in DMEM/F12. Cell numbers were counted using a Cellometer (Nexelom Bioscience, Lawrence, MA).

To harvest urethral epithelium, 10-week-old adult C57BL/6 male mice were used as donors as they are postpubescent and thus beyond tissue morphogenesis and within homeostatic tissue maintenance. The urethra was isolated and the muscle layer was manually teased off. The epithelial sheath was transferred into DMEM/F12 medium and digested into a single cell suspension using 0.2% collagenase as described above.

To induce human prostate glands, CMDM cells or UGSM cells were mixed with hESCs at a 1:2.5 ratio of hES/mesenchymal cells. The cell mixtures were re-suspended with 75% Matrigel (BD Biosciences) and injected into the subrenal capsule of adult male nude mice. As controls, CMDM cells, UGSM cells, and hESCs were grafted alone into adult male nude mouse hosts. After 10 weeks, glandular tissues were harvested and analyzed. To induce mouse prostate glands, either CMDM cells or UGSM cells were mixed with adult mouse urethral epithelial cells at a 1:2.5 ratio of epithelial/mesenchymal cells and implanted as described above.

Tissue collection, preparation, and prostate microdissection

After euthanasia, the urogenital tract was dissected from the surrounding tissues, removed en bloc including the urethra, all prostate lobes, two seminal vesicles, and bladder, and photographed. To dissect prostatic lobes, the mouse prostate was dissociated using 0.2% collagenase (type IV; Sigma) for 15 min. The tissue was gently teased using needles under a dissection microscope (Leica MZ16F stereomicroscope) and photographed. The tissues were embedded in 2% agar gel with optimal orientation and then embedded in paraffin and serially sectioned. Tissue samples were processed by the University of Chicago Human Tissue Resource Core facility. Briefly, tissue samples were formalin-fixed for 24 h and embedded in paraffin immediately after necropsy. Sections (5 μm thick) were adhered to positively charged slides.

Histology and immunostaining

H&E staining was performed using a SAKURA Tissue-Tek Prima Autostainer. For immunohistochemistry staining, formalin-fixed, paraffin-embedded slides were deparaffinized in xylene, and hydrated using graded ethanol washes. Tissues

were treated with antigen retrieval buffer (S1699 from DAKO, Glostrup, Denmark) in a steamer for 20 min. Anti-p63 (D2K8X rabbit monoclonal; Cell Signaling Technology, Danvers, MA) and anti-AR (N-20 rabbit polyclonal; Santa Cruz Biotechnology, Santa Cruz, CA) were applied for 1 h at room temperature in a humidity chamber. Following TBS wash, the antigen-antibody binding was detected with Envision+system (K4001; DAKO, Carpinteria, CA) and DAB+Chromogen (K3468; DAKO). Tissue sections were briefly immersed in hematoxylin for counterstaining and were cover-slipped. For immunofluorescence staining, after deparaffinization and rehydration, tissues were treated with heat-induced antigen retrieval using Tris-EDTA buffer (10 mM Tris Base, 1 mM EDTA Solution, pH 9.0) in a pressure cooker for 3 min. After 30 min of blocking in 10% normal goat serum phosphate-buffered saline (PBS), slides were incubated with primary antibodies followed by secondary Alexa Fluor goat anti-rabbit IgG or/and anti-mouse IgG (Cell Signaling). Following PBS wash, the tissues were counterstained with DAPI and were cover-slipped.

Antibodies used for immunostaining were AR (N20, rabbit polyclonal, 1:400; Santa Cruz Biotechnologies), p63 (4A4, mouse monoclonal, 1:100; Santa Cruz Biotechnologies), NKX3.1 (rabbit polyclonal, 1:50; Biocare), HOXB13 (H-80, rabbit polyclonal, 1:100; Santa Cruz Biotechnologies), chromogranin A (LK2H10, mouse monoclonal, 1:100; Santa Cruz Biotechnologies), and PSA (C-19, goat polyclonal, 1:100; Santa Cruz Biotechnologies). DAPI (1:1,000; Invitrogen) was used to counterstain the nucleus. Secondary staining reagents included Alexa Fluor goat anti-rabbit IgG (Cell Signaling Technologies), Alexa Fluor goat anti-mouse IgG (Cell Signaling Technologies), or Alexa Fluor donkey anti-goat IgG (Invitrogen).

Colorimetric images were captured using a Panoramic Scan Whole Slide Scanner (Cambridge Research and Instrumentation, Hopkinton, MA) and images captured using the Panoramic Viewer software version 1.14.50 (3DHistech; Budapest, Hungary). For immunofluorescence staining slides, images were captured using an Olympus FV1000 laser scanning confocal microscope.

Results

Transcription factors used to differentiate between prostate and urethral epithelia

To elucidate the differences between the prostate and urethral glands, we analyzed the expression of transcriptional factors associated with epithelial (ΔNp63), genitourinary (AR), or prostatic lineage (NKX3.1 and HOXB13) using both human and mouse tissues (Fig. 1a, c). ΔNp63 is a basal-restricted transcription factor that is necessary for prostate development and maintenance of basal epithelial cells in bi-layered epithelia, which include both the urethral and prostate glands [9,10]. AR is a central steroid transcription factor with a well-documented and important role in prostate genitourinary development, prostate homeostasis, and prostate cancer [2,11]. Urethral glands also contain nuclear AR and are therefore responsive to testosterone [12]. NKX3.1 is an androgen-induced homeobox transcriptional factor that regulates organogenesis and epithelial differentiation of the prostate [13–15]. NKX3.1 is expressed early in the male urogenital epithelium, and its presence indicates induction of prostatic epithelial identity [2,16]. Genetic lineage tracing has demonstrated that NKX3.1^{+} cells can reconstitute all three lobes of the rodent prostate in renal capsule experiments [17]. HOXB13 is another homeobox

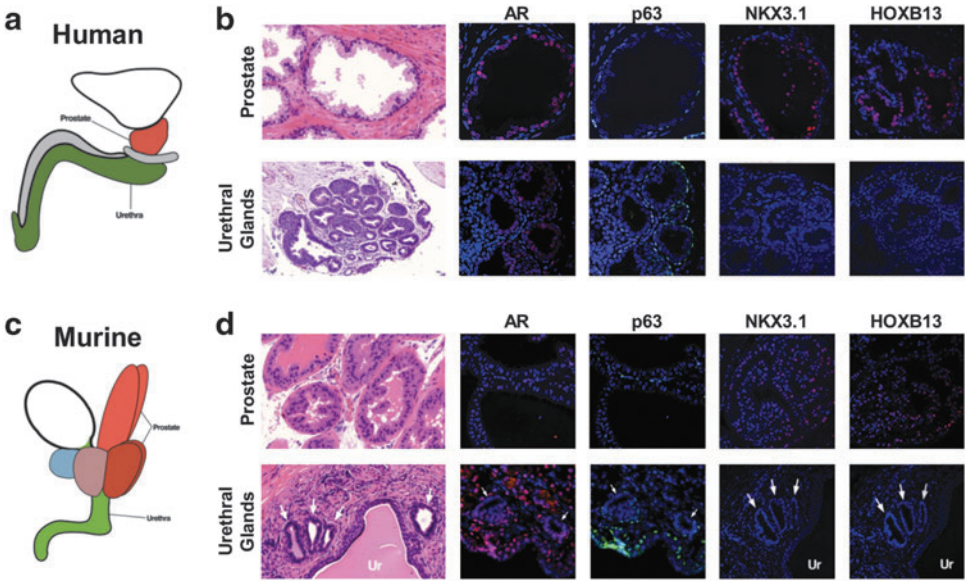

FIG. 1. NKX3.1 and Hoxb13 expression in prostate but not urethral gland epithelia. **(a, c)** Schematic depicting the anatomy of the human prostate (*red*), urethra (*green*), and bladder (*white*). **(b)** H&E staining and IF staining of AR, ΔNp63 (p63), NKX3.1, and HOXB13 in human prostate and urethral glands. **(d)** H&E staining and IF staining of AR, p63, NKX3.1, and Hoxb13 in the murine urethral and prostate glands. UR indicates urothelium. NKX3.1 and HOXB13 are seen in the human and murine prostate but not in the neighboring urethral gland epithelia. *Arrows* indicate urethral glands located by the urethra. AR, androgen receptor; H&E, hematoxylin and eosin; IF, immunofluorescence.

transcriptional factor that is critical in prostate development and adult organ function and mutations in HOXB13 are associated with a subset of familial prostate tumors [18–21]. HOXB13 is commonly used as a persistent marker of terminally differentiated prostatic luminal epithelium. During fetal development, the UGS contributes to the development of the bladder, urethra, and prostate. Urethral epithelial cells branch off to form the urethral glands, and are located along the urethra. However, at the proximal region of the urethra, some epithelial ducts grow beyond the urethral wall and repeatedly branch to form prostate acini [6,22].

As expected, both human and mouse prostate epithelium and urethral gland epithelium contain ΔNp63-positive basal cells and AR-positive luminal cells (Fig. 1b, d) [23]. Human and mouse prostate luminal cells express NKX3.1 and HOXB13, however, urethral gland epithelial cells lack both NKX3.1 and HOXB13 expression (Fig. 1b, d). Given the common derivation of both prostate and urethral epithelial cells from the UGS, we sought to investigate how these divergent epithelial structures formed, and the role of stroma in determining their cell fate.

Transcription factor expression analyses highlight decision point for urethral and prostatic epithelium

To determine at what point during development the UGS epithelium gives rise to distinct urethral and prostate epithelia, we followed the expression of ΔNp63, HOXB13, and NKX3.1 during mouse prostate development (Fig. 2a). First, we analyzed protein expression of the mouse UGS at embryonic day (E) 11.5, when the urorectal septum separates the UGS anteriorly from the hindgut posteriorly (Figs. 2a and 3a) [4]. HOXB13 is sparsely seen in epithelial cells of the UGS, but uniformly expressed in the hindgut epithelium (Fig. 2b). As expected, the majority of UGS epithelial cells express ΔNp63 (Fig. 2b), as it has been previously shown to be required for differentiation of the urogenital tract and inhibits differentiation toward the intestinal epithelium [24,25]. In contrast, hindgut epithelial cells lack p63 expression (Fig. 2b). At E14.5, ΔNp63 was expressed in the whole UGS epithelium, while HOXB13 expression is observed in a small area of upper UGS (Fig. 3b). At E17.5, HOXB13 expression is undetectable in all UGS epithelial cells, while there is robust expression in the epithelial cells of the colon (Fig. 2c). By postnatal day 5 (P5), HOXB13 is detected in the prostate, but absent in the urothelium, urethral glands, and the urethral portion of the prostatic ducts (Fig. 3c).

Previous studies documented that NKX3.1 mRNA is first detected in the UGS epithelium at E15.5 [26]. However, we did not observe NKX3.1 protein expression in serial sections of mouse UGS tissues at E15.5 (Supplementary Fig. S1a; Supplementary Data are available online at www.liebertpub.com/scd). The earliest prostatic buds are seen at E16.5 and coincide with detectable NKX3.1 protein expression (Fig. 2d). Notably, NKX3.1 is only detectable in epithelial buds, while the UGS epithelium lacked NKX3.1 expression (Fig. 2d). At E17.5, prostatic buds are more prevalent, and NKX3.1 expression remains in prostate epithelial ducts while remaining absent in the UGS epithelium (Fig. 2e). As the urethral shape gradually matures, the prostate ducts extend and grow outside

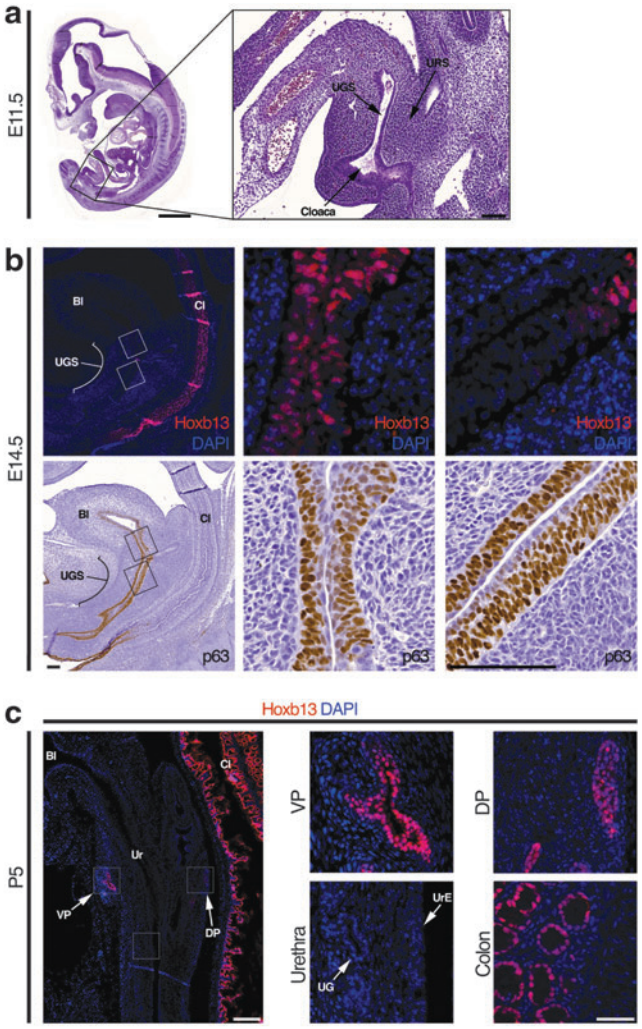

FIG. 2. Cell fate transition during development of the UGS. **(a)** H&E staining of sagittal-sectioned E11.5 mouse embryo. **(b)** IF staining of Hoxb13 and immunohistochemistry staining of p63 in E14.5 mouse embryo. **(c)** IF staining for Hoxb13 in postnatal day 5 prostate, ventral prostate, dorsal prostate, urethra, and colon. Bl, bladder; Cl, colon; UGS, urogenital sinus; URS, urorectal septum.

the urethral wall and are clearly demarcated by NKX3.1 expression (Supplementary Fig. S1b). The appearance and maintained expression of NKX3.1 and Hoxb13 in prostate epithelial buds, and distinct lack of expression in urethral glands, suggest that there are key differences in the stromal microenvironment that promote transcription factor expression and prostate lineage specification.

CMDM is sufficient to specify prostatic epithelial cell fate

The common origin of prostate and urethral epithelial cells implies that different stromal cues dictate the lineage of each gland during development. During embryogenesis, the Wolffian duct (WD) and the MD converge in the region where the prostatic buds initiate [4]. In men, the ejaculatory ducts are derived from the WD and pass through the prostate, and lack expression of neither HOXB13 nor NKX3.1

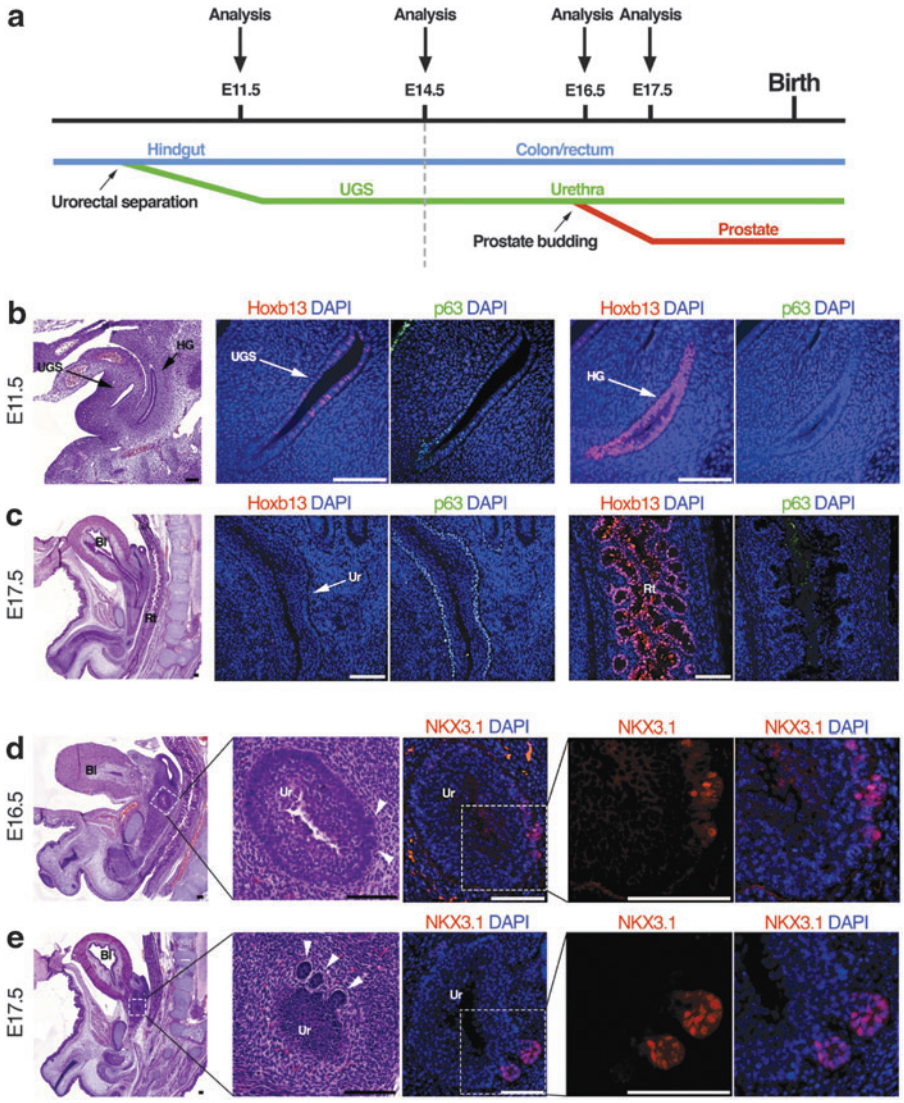

FIG. 3. Sequential analyses of prostate and urethral gland development from the HG to UGS to the prostate. **(a)** Schematic depicting development of the UGS and time points when analyses of transcription factors were performed. **(b)** H&E staining and IF staining of Hoxb13 and p63 in the UGS and HG of E11.5 mouse embryo. **(c)** H&E staining and IF staining of Hoxb13 and p63 in the Ur, Rt, and Bl of E17.5 mouse embryo. *Arrows* indicate regions of interest. **(d, e)** H&E staining and IF staining of NKX3.1 in the urethra of E16.5 and E17.5 mouse embryos documenting prostatic budding. *Arrowheads* mark prostatic buds. Scale bars represent 100 μm. Bl, bladder; HG, hindgut; Rt, rectum; Ur, urethra.

(Supplementary Fig. S1c), supporting that the WD mesenchyme does not induce prostatic cell lineage specification. We have previously hypothesized that the CMDM) participates in prostate development [6]. This is based upon the observation that, although the MD regresses in the male due to the presence of AMH, the middle portion of the MD undergoes regression via epithelial-mesenchymal transition [27–29]. Thus, a portion of Müllerian Duct Mesenchyme (MDM) may persist and induce prostate development. Further supporting the role of MDM in prostate development is the expression pattern of AR in MDM and therefore the potential to secrete paracrine growth factors in response to host androgens (Supplementary Fig. S2).

To directly test the ability of MDM to promote prostate epithelial development, we utilized a tissue recombination approach whereby hESCs are induced by embryonic rodent stroma to form human prostate glands [8,30]. The CMDM includes the cervix and upper vagina and was derived from female rat neonates (Fig. 4a). The UGSM was used as a control stroma, and was harvested from the urethra of female rat neonates; male UGSM was not used due to the potential contamination of adjoining caudal MD. We reconstituted hESCs with either CMDM cells or UGSM cells from female rat neonates; these recombinants were implanted under the renal capsule of adult male nude mice (Fig. 4a). After a growth period of 12 weeks, both CMDM- and UGSM-induced glands had a continuous p63-positive basal cell layer (Fig. 4b). Control hESCs implanted alone formed teratomas as expected, and mesenchyme implanted without hESCs did not yield any tissue for analyses after 12 weeks. Both CMDM and UGSM-induced glands expressed AR and human-restricted PSA, demonstrating human origin of tissues and a lack of contaminating mouse epithelium (Supplementary Fig. S3a, b). As further confirmation of the formation of multiple cell lineages, hESC-derived glands contained chromogranin A-expressing neuroendocrine cells (Supplementary Fig. S3c). Significantly, the luminal cells within CMDM-induced glands expressed NKX3.1, while UGSM-induced glands lacked NKX3.1 expression (Fig. 4b). Neither CMDM nor UGSM-induced epithelia, however, expressed detectable HOXB13 protein (Fig. 4b). These data support our hypothesis that the caudal MD is sufficient to induce prostate epithelial cell lineage specification as documented by the expression of human-specific PSA and NKX3.1.

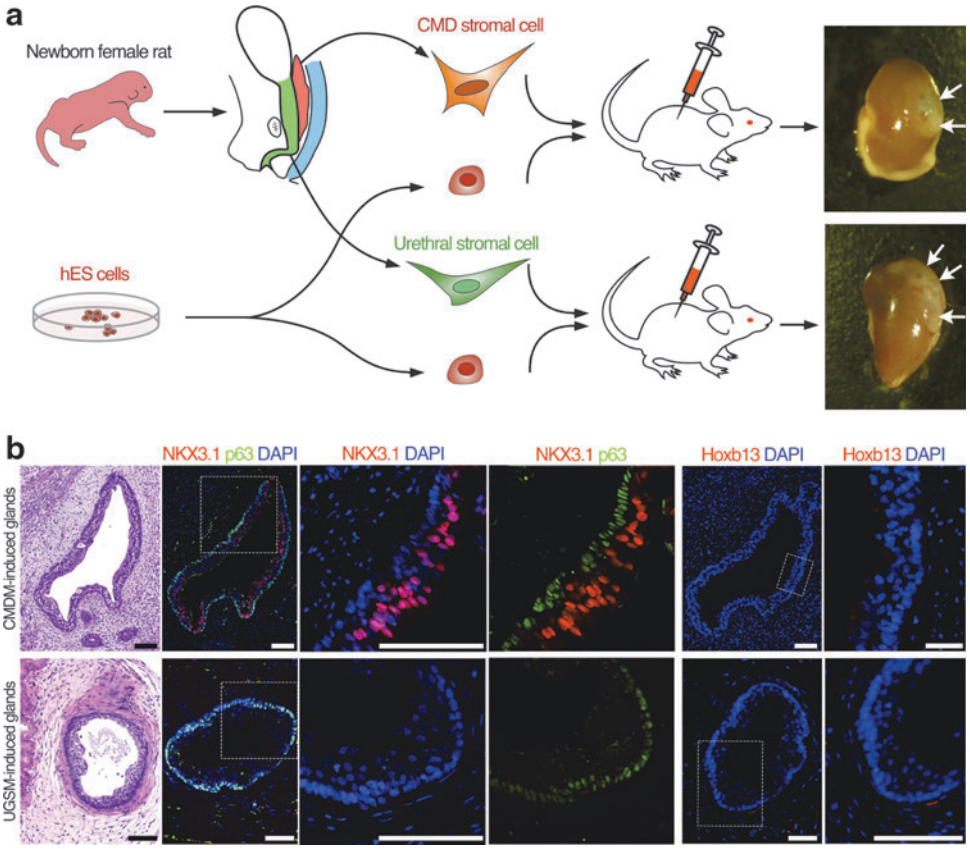

FIG. 4. CMDM induces partial prostatic cell fate in glands derived from hESCs. **(a)** Diagram shows tissue recombination approach using hESCs. hESCs were mixed with either caudal MD stromal cells or urethral stromal cells from newborn female rats. *Arrows* mark tissue recombinants underneath the mouse renal capsule. **(b)** H&E staining and IF staining of NKX3.1, HOXB13, and p63 in the hESC-derived glands induced by rat CMDM cells or rat UGSM cells. These data demonstrate induction of NKX3.1-positive epithelia indicative of prostate, but such tissue lacks HOXB13 expression indicating incomplete prostatic fate determination. Scale bars represent 100 μm. CMDM, caudal Müllerian duct mesenchyme; hESC, human embryonic stem cell; MD, Müllerian duct; UGSM, urogenital sinus mesenchyme.

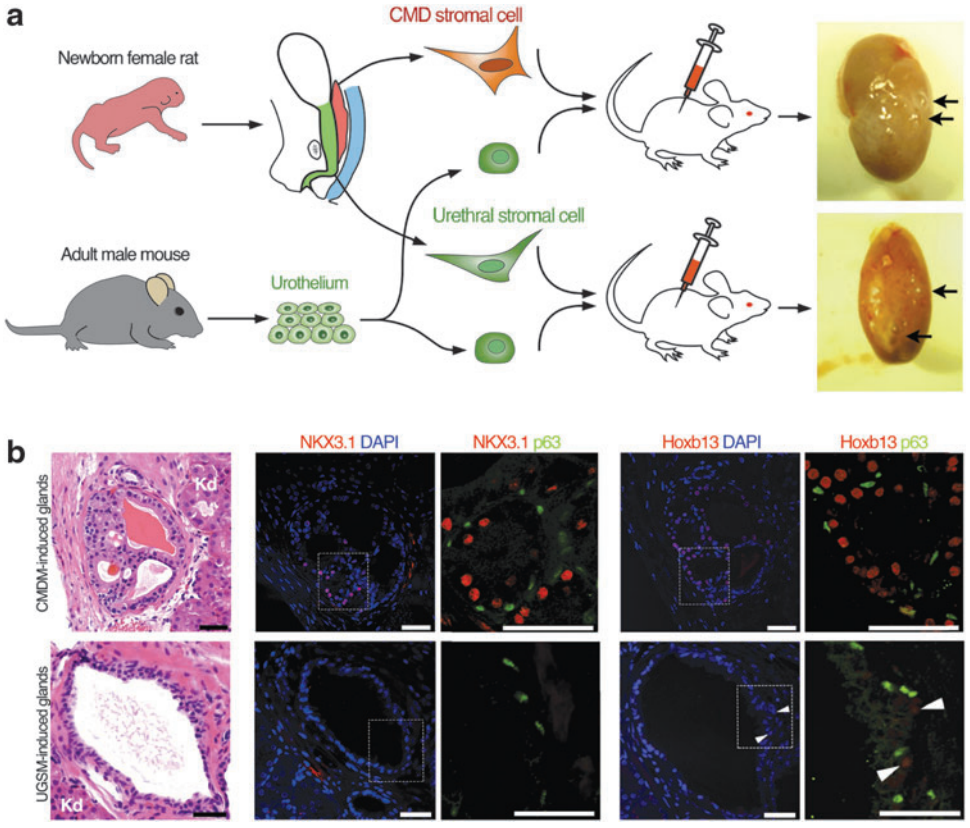

FIG. 5. CMDM induces prostate cell fate in urothelial cell-derived glands. **(a)** Diagram shows tissue recombination using adult mouse urothelial cells. *Arrows* mark the tissue recombinants underneath the mouse renal capsule. Urothelial cell epithelia from adult male mice was recombined with either caudal MD stromal cells or urethral stromal cells from newborn female rats. **(b)** H&E staining and IF staining of NKX3.1, HOXB13, and p63 in the urothelium-derived glands induced by rat CMDM cells or rat UGSM cells. *Arrowheads* mark sporadic expression of HOXB13. These data demonstrate that recombination of adult urothelium and caudal MD generates prostatic epithelium that is positive for both NKX3.1 and HOXB13. Scale bars, 50 μm. Kd, kidney.

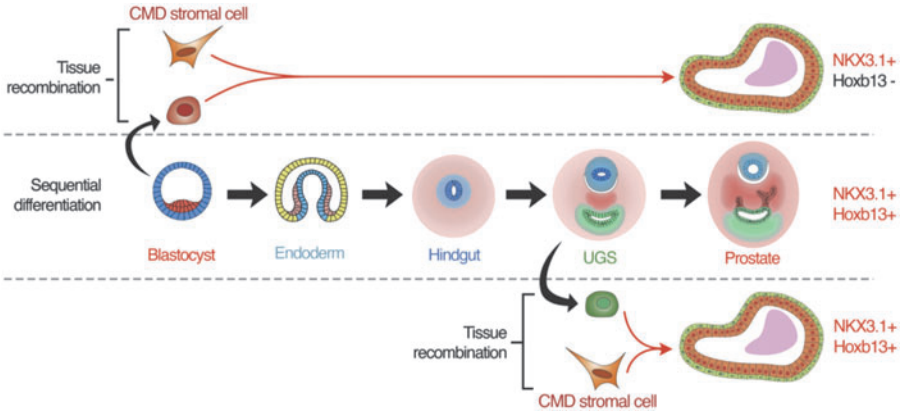

FIG. 6. Diagram of prostatic cell fate and role of CMDM. Diagram shows the differences among the sequential differentiation and tissue recombinations using either pluripotent embryonic stem cells or urothelial cells as the originating epithelial cell precursor.

Maintenance of HOXB13 expression by caudal MD but not UGSM

When hESCs were used for human prostate epithelium induction, glandular structures induced by CMDM or UGSM lacked HOXB13 expression (Fig. 4b). We hypothesized that this was due to the use of pluripotent hESCs to form human prostate epithelium, which are more primitive than hindgut epithelium from which prostatic epithelium is derived and therefore may not have been conditioned properly to be able to express HOXB13. It is possible that the expression of HOXB13 is not initiated by but maintained by the mechanism that separates prostatic from urethral epithelia. To test this, we harvested urethral epithelium from adult mice and reconstituted them with either CMDM cells or UGSM cells from female rat neonates (Fig. 5a). Indeed, luminal cells within glands induced by CMDM express both NKX3.1 and HOXB13, while glands induced by UGSM lack expression of both transcriptional factors (Fig. 5b). These data demonstrate that HOXB13 expression in the prostatic epithelium is maintained after differentiation into hindgut epithelium, and implies that UGSM suppresses HOXB13 in urethral gland epithelia while the CMDM maintains HOXB13 expression (Fig. 5b). Taken together, these data demonstrate that the CMDM is able to specify the formation of prostate epithelial cells. During this process, the CMDM induces the expression of NKX3.1, and maintains the expression of HOXB13 to contribute to the delineation of prostate epithelium from urethral epithelium (Fig. 6). These data strongly implicate a key role for the caudal MD in specifying prostate lineage from urethral gland lineage.

Discussion

In this study we provide evidence that the CMDM is able to induce prostate epithelia and is likely a key determinant in delineating prostate versus urethral gland cell fate. This is in contrast to the conventional belief that the prostate is induced solely by the UGSM. Our data are significant for three reasons. First, the ability of MDM to induce prostate formation helps explain a long-standing observation that vaginal stroma is able to induce prostate epithelium formation, and even high-dose testosterone treatment in postpartum females can result in prostate formation [31]. Second, our data help to elucidate how a common embryonic structure, the UGS, can be influenced by stroma to form both urethral and prostate epithelium. Third and finally, given the vast disparity in disease incidence between the prostate and urethral gland epithelium, our data provide a rationale for future investigations into whether the CMDM could be a potential mediator in prostate neoplasia and cancer initiation; such MDM-derived paracrine factors have the potential to become novel targets for prostate cancer prevention or therapeutic intervention. A limitation of our study is that the use of adult urethra epithelial cells may be a poor substitute for the embryonic UGS epithelial cells, or adult prostate stem cells, that give rise to the prostatic epithelium. Future studies should be aimed at understanding the relationship between CMDM and UGSM into adult prostate homeostasis and their impact on prostate epithelium and responses to androgen deprivation.

In the developing male urogenital tract, it has long been presumed that AMH inhibits the MD epithelial cells to develop the female reproductive organs. However, the fate of the MD mesenchyme is unclear. Our data support a model whereby androgens induce the CMDM to develop into prostate, thereby highlighting a sexual dimorphic differentiation of the CMDM. MD-derived glands have been found in males of lower vertebrates such as amphibians [32,33] and play roles in improving fertility by increasing sperm velocity and providing nutrients [34]. Thus, our findings suggest that factors derived from the CMDM-derived stroma could serve as efficacious targets for cancer prevention and initiation. The identification of such targets using comparative approaches and additional functional studies is an obvious area for future research.

Acknowledgments

We wish to acknowledge the support of the University of Chicago Section of Urology led by Dr. Arieh Shalhav. We would also like to acknowledge the support of the University of Chicago Comprehensive Cancer Center (UCCCC) led by Dr. Michelle Le Beau. We also thank Dr. Yi Cai for the superb technical assistance on the project. We also wish to thank the expert technical assistance of the Human Tissue Resource Center core facility led by Dr.

Mark Lingen, and the assistance of Mary Jo Fekete. We also thank the Immunohistochemistry Core Facility run by Terri Li. NIH RO1CA178431 (D.J.V.G.); DOD PCRP PC130587 (D.J.V.G.); the University of Chicago Comprehensive Cancer Center (UCCCC), especially the Cancer Center Support Grant (P30CA014599); an American Cancer Society Institutional Research Grant (ACS-IRG, No. IRG-58-004; D.J.V.G.); an Anonymous Foundation, The Brinson Foundation; the Alvin Baum Family Fund; The Pierce Foundation; The University of Chicago Cancer Research Foundation Women's Board; H.B. was supported by the Cancer Biology Training Grant (T32 CA 009594); E.M.M. was supported by the Molecular and Cellular Biology Training Grant (T32 GM007183).

Author Disclosure Statement

No competing financial interests exist.

References

1. Chung LW and GR Cunha. (1983). Stromal-epithelial interactions: II. Regulation of prostatic growth by embryonic urogenital sinus mesenchyme. Prostate 4:503–511.
2. Cunha GR, W Ricke, A Thomson, PC Marker, G Risbridger, SW Hayward, YZ Wang, AA Donjacour and T Kurita. (2004). Hormonal, cellular, and molecular regulation of normal and neoplastic prostatic development. J Steroid Biochem Mol Biol 92:221–236.
3. McNeal JE. (1981). The zonal anatomy of the prostate. Prostate 2:35–49.
4. Timms BG. (2008). Prostate development: a historical perspective. Differentiation 76:565–577.
5. Cunha GR and LW Chung. (1981). Stromal-epithelial interactions—I. Induction of prostatic phenotype in urothelium of testicular feminized (Tfm/y) mice. J Steroid Biochem 14:1317–1324.
6. Cai Y. (2008). Participation of caudal mullerian mesenchyma in prostate development. J Urol 180:1898–1903.
7. Kurita T. (2010). Developmental origin of vaginal epithelium. Differentiation 80:99–105.
8. Cai Y, S Kregel and DJ Vander Griend. (2013). Formation of human prostate epithelium using tissue recombination of rodent urogenital sinus mesenchyme and human stem cells. J Vis Exp 76:50327.
9. Barbieri CE and JA Pietenpol. (2006). p63 and epithelial biology. Exp Cell Res 312:695–706.
10. Grisanzio C and S Signoretti. (2008). p63 in prostate biology and pathology. J Cell Biochem 103:1354–1368.
11. Litvinov IV, AM De Marzo and JT Isaacs. (2003). Is the Achilles' heel for prostate cancer therapy a gain of function in androgen receptor signaling? J Clin Endocrinol Metab 88:2972–2982.
12. Yang YA and J Yu. (2015). Current perspectives on FOXA1 regulation of androgen receptor signaling and prostate cancer. Genes Dis 2:144–151.
13. Tanaka M, I Komuro, H Inagaki, NA Jenkins, NG Copeland and S Izumo. (2000). Nkx3.1, a murine homolog of Ddrosophila bagpipe, regulates epithelial ductal branching and proliferation of the prostate and palatine glands. Dev Dyn 219:248–260.
14. Abate-Shen C, MM Shen and E Gelmann. (2008). Integrating differentiation and cancer: the Nkx3.1 homeobox gene in prostate organogenesis and carcinogenesis. Differentiation 76:717–727.
15. Matusik RJ, RJ Jin, Q Sun, Y Wang, X Yu, A Gupta, S Nandana, TC Case, M Paul, et al. (2008). Prostate epithelial cell fate. Differentiation 76:682–698.
16. Hutmacher DW, BM Holzapfel, EM De-Juan-Pardo, BA Pereira, SJ Ellem, D Loessner and GP Risbridger. (2015). Convergence of regenerative medicine and synthetic biology to develop standardized and validated models of human diseases with clinical relevance. Curr Opin Biotechnol 35:127–132.
17. Thorne RM and TA Milne. (2015). Dangerous liaisons: cooperation between Pbx3, Meis1 and Hoxa9 in leukemia. Haematologica 100:850–853.
18. Economides KD and MR Capecchi. (2003). Hoxb13 is required for normal differentiation and secretory function of the ventral prostate. Development 130:2061–2069.
19. Ewing CM, AM Ray, EM Lange, KA Zuhlke, CM Robbins, WD Tembe, KE Wiley, SD Isaacs, D Johng, et al. (2012). Germline mutations in HOXB13 and prostate-cancer risk. N Engl J Med 366:141–149.
20. Akbari MR, J Trachtenberg, J Lee, S Tam, R Bristow, A Loblaw, SA Narod and RK Nam. (2012). Association between germline HOXB13 G84E mutation and risk of prostate cancer. J Natl Cancer Inst 104:1260–1262.
21. Huang Q, T Whitington, P Gao, JF Lindberg, Y Yang, J Sun, MR Vaisanen, R Szulkin, M Annala, et al. (2014). A prostate cancer susceptibility allele at 6q22 increases RFX6 expression by modulating HOXB13 chromatin binding. Nat Genet 46:126–135.
22. Wilson JD. (2011). The critical role of androgens in prostate development. Endocrinol Metab Clin North Am 40: 577–590, ix.
23. Cohen RJ, K Garrett, JL Golding, RB Thomas and JE McNeal. (2002). Epithelial differentiation of the lower urinary tract with recognition of the minor prostatic glands. Hum Pathol 33:905–909.
24. Signoretti S, D Waltregny, J Dilks, B Isaac, D Lin, L Garraway, A Yang, R Montironi, F McKeon and M Loda. (2000). p63 is a prostate basal cell marker and is required for prostate development. Am J Pathol 157:1769–1775.
25. Signoretti S, MM Pires, M Lindauer, JW Horner, C Grisanzio, S Dhar, P Majumder, F McKeon, PW Kantoff, WR Sellers and M Loda. (2005). p63 regulates commitment to the prostate cell lineage. Proc Natl Acad Sci U S A 102: 11355–11360.
26. Bhatia-Gaur R, AA Donjacour, PJ Sciavolino, M Kim, N Desai, P Young, CR Norton, T Gridley, RD Cardiff, et al. (1999). Roles for Nkx3.1 in prostate development and cancer. Genes Dev 13:966–977.
27. Allard S, P Adin, L Gouedard, N di Clemente, N Josso, MC Orgebin-Crist, JY Picard and F Xavier. (2000). Molecular mechanisms of hormone-mediated Mullerian duct regression: involvement of beta-catenin. Development 127:3349–3360.
28. Zhan Y, A Fujino, DT MacLaughlin, TF Manganaro, PP Szotek, NA Arango, J Teixeira and PK Donahoe. (2006). Mullerian inhibiting substance regulates its receptor/SMAD signaling and causes mesenchymal transition of the coelomic epithelial cells early in Mullerian duct regression. Development 133:2359–2369.
29. Klattig J, R Sierig, D Kruspe, B Besenbeck and C Englert. (2007). Wilms' tumor protein Wt1 is an activator of the

anti-Mullerian hormone receptor gene Amhr2. Mol Cell Biol 27:4355–4364.
30. Taylor RA, PA Cowin, GR Cunha, M Pera, AO Trounson, J Pedersen and GP Risbridger. (2006). Formation of human prostate tissue from embryonic stem cells. Nat Methods 3: 179–181.
31. Cunha GR. (1975). Age-dependent loss of sensitivity of female urogenital sinus to androgenic conditions as a function of the epithelia-stromal interaction in mice. Endocrinology 97:665–673.
32. Wake MH. (1981). Structure and function of the male Mullerian gland in caecilians, with comments on its evolutionary significance. J Herpetol 15:17–22.
33. Sever DM. (1991). Comparative anatomy and phylogeny of the cloacae of salamanders (Amphibia: Caudata). I. Evolution at the family level. Herpetologica 47:165–193.
34. George JM, M Smita, B Kadalmani, R Girija, OV Oommen and MA Akbarsha. (2005). Contribution of the secretory material of caecilian (amphibia: Gymnophiona) male Mullerian gland to motility of sperm: a study in *Uraeotyphlus narayani*. J Morphol 263:227–237.

Address correspondence to:
Dr. Donald J. Vander Griend
Department of Surgery
Section of Urology
The University of Chicago
5841 South Maryland Avenue
MC6038
Chicago, IL 60637

E-mail: prostate@uchicago.edu

Received for publication April 18, 2016
Accepted after revision September 5, 2016
Prepublished on Liebert Instant Online September 5, 2016